Resonant Germanium Nanoantenna Photodetectors

ARTICLE *in* NANO LETTERS · MARCH 2010

Impact Factor: 13.59 · DOI: 10.1021/nl9037278 · Source: PubMed

NANO LETTERS

pubs.acs.org/NanoLett

Resonant Germanium Nanoantenna Photodetectors

Linyou Cao,[†] Joon-Shik Park,[†,‡] Pengyu Fan,[†] Bruce Clemens,[†] and Mark L. Brongersma*[,†]

[†]Geballe Laboratory for Advanced Materials, Stanford University, California 94305 and [‡]Nanomechatronics Research Center, Korea Electronics Technology Institute, Gyeonggi, 463-816, Republic of Korea

ABSTRACT On-chip optical interconnection is considered as a substitute for conventional electrical interconnects as microelectronic circuitry continues to shrink in size. Central to this effort is the development of ultracompact, silicon-compatible, and functional optoelectronic devices. Photodetectors play a key role as interfaces between photonics and electronics but are plagued by a fundamental efficiency−speed trade-off. Moreover, engineering of desired wavelength and polarization sensitivities typically requires construction of space-consuming components. Here, we demonstrate how to overcome these limitations in a nanoscale metal−semiconductor−metal germanium photodetector for the optical communications band. The detector capitalizes on antenna effects to dramatically enhance the photoresponse (>25-fold) and to enable wavelength and polarization selectivity. The electrical design featuring asymmetric metallic contacts also enables ultralow dark currents (~20 pA), low power consumption, and high-speed operation (>100 GHz). The presented high-performance photodetection scheme represents a significant step toward realizing integrated on-chip communication and manifests a new paradigm for developing miniaturized optoelectronics components.

KEYWORDS Photodetector, antenna, Mie resonance, nanophotonics, nanowire

Ge is considered to be one of the most promising materials for near-infrared (1.3−1.6 μm) photodetectors in integrated optical circuits because of its large absorption coefficient (related to its direct gap at 0.8 eV) and compatibility with standard silicon-processing technology.[1−4] Substantial resources have been devoted to develop compact on-chip Ge photodetectors featuring high speed and responsivity.[5−12] For example, detector elements have been embedded in optical resonators to enhance responsivity[7] and waveguide-based detectors have been developed to get around the infamous efficiency-speed trade-off.[5,6,10] Unfortunately, these structures offer limited opportunities for scaling, and seamless integration with nanoscale electronic components is precluded. Nanometallic (i.e., plasmonic) light concentration structures have enabled further shrinking of device dimensions below the diffraction limit and absorption depth of a semiconductor without significant loss in responsivity.[9,11] However, one would ideally avoid the intrinsic heating losses in metals.

Another desirable feature attracting significant attention is the integration of wavelength and polarization selectivity into photodetectors that usually only sense the signal intensity.[13−16] This would facilitate communication encoded in polarization states of light[17] and valuable demultiplexing of wavelength division multiplexed (WDM) signals, greatly extending the available bandwidth of optical interconnection.[18] Efforts to increase functionality again require the use of bulky external structures,[9,13−16] akin to the attempts to enhance responsivity. Polarization and wavelength selective detection has been realized by adding filters capable of screening specific polarization or wavelength of light, including grating couplers,[13] wire grid polarizers,[16] interdigitated metallic electrodes,[14] or planar cavities.[15] Here, we for the first time propose a photodetector that combines the strong intrinsic optical resonance effects in semiconductor nanowires with the excellent high-speed, low-noise performance of metal−semiconductor−metal (MSM) photodetectors. We demonstrate that the resonances can be engineered to boost the absorption of light in a CMOS-compatible Ge nanowire-based MSM detector by over ~25-fold compared to nonresonant designs. The nature of the resonance also naturally offers polarization and wavelength selectivity at the important 1.55 μm communication wavelength. Owing to its small dimension and the use of asymmetric metal contacts (one side Ohmic and the other Schottky), the photodetector also features a very low dark current, can work at zero bias, and is expected to have very high operation speed (>100 GHz).

It was recently shown that semiconductor nanowires (NWs) can exhibit a strongly enhanced and tunable photoresponse.[19−22] Physically, the enhanced light−matter interaction arises from the coupling of incident light to leaky mode resonances (LMRs) supported by the nanowires;[19] sufficiently large NWs can be thought of as a cylindrical cavity antenna[23] that can trap light in circulating orbits by multiple total internal reflections from the periphery, as illustrated in Figure 1a upper inset. It is worth noting that planar detectors exploiting Fabry−Pérot resonances in thin films are expected to experience smaller field enhancements than wire detectors as they rely on relatively weak reflections at normal incidence. To exploit the LMRs achieving optimal photodetection performance at near-infrared wavelengths,

* To whom correspondence should be addressed, brongersma@stanford.edu.
Received for review: 11/6/2009
Published on Web: 03/15/2010

DOI: 10.1021/nl9037278 | *Nano Lett.* **2010,** *10,* 1229–1233

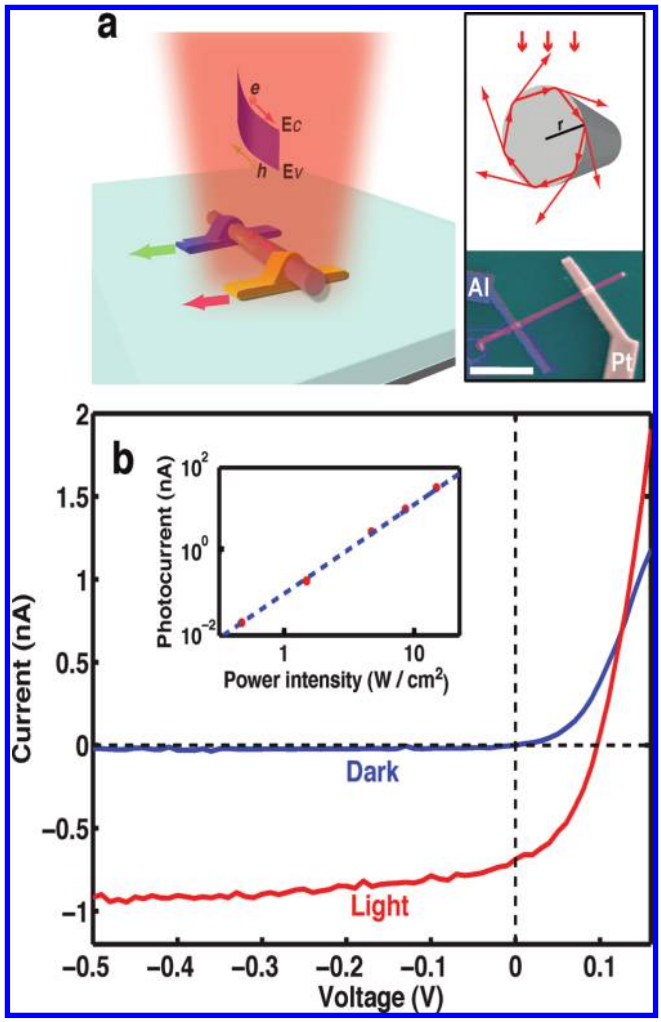

FIGURE 1. Schematics and electrical characterization of a germanium (Ge) nanowire-based MSM photodetector. (a) Ge nanowire photodetector with asymmetric (one side Ohmic and the other Schottky) metallic contacts: upper inset, illustration of the optical antenna effect in nanowires; lower inset, SEM image of a typical nanowire device (scale bar is 1 μm). (b) Dark and light $I-V$ curves of a typical nanowire device. Inset, dependence of the photoresponse of the nanowire photodetector on incident power, which closely follows a linear fit to the data (dashed blue line).

we propose a photodetector structure as drawn in Figure 1a. The photodetector is composed of an intrinsically grown Ge nanowire using a chemical vapor deposition process,[24] and electrical contacts (2 nm of Ti/400 nm of Al and 5 nm of Cr/400 nm of Pt) were defined at both ends with standard e-beam lithography, metal deposition, and lift-off techniques. The light absorption by the NW was designed to be resonant at a specifically desired near-infrared wavelength, for example, 1550 nm. The electrode metals were chosen to form an asymmetric MSM detector with one Schottky and one Ohmic contact; this type of asymmetric structure was shown effective in suppressing dark current while facilitating collection of photogenerated charge carriers.[25] Figure 1a lower inset shows a scanning electron microscopy (SEM) image of a typical device.

Characteristic current−voltage ($I-V$) curves of the nanowire device are given in Figure 1b. The $I-V$ curve exhibits rectifying behavior, confirming that the device is a well-behaved diode structure with the electric contact on one side (Al) Ohmic and the other (Pt) Schottky. The reverse bias dark current of the device is very small, ∼20 pA at −1 V, and could be further improved by properly passivating the GeNW surface. Upon illumination, the device shows a pronounced photovoltaic response due to the built-in potential from the Schottky junction. The short length of the nanowire device and the large depleted region by the built-in potential enable the nanowire photodetector to be operated at *zero* bias. Figure 1b shows the photocurrent of the device at *zero* bias as a function of irradiance. The linearity of the device was demonstrated up to at least ∼20 W/cm^2 at a 632 nm wavelength (limited by our current experimental setup). The excellent linear response is in part based on the good crystalline quality of the nanowires, as confirmed by transmission electron microscopy (not shown). In addition, the capacitance of a typical device (∼1−2 μm in length and ∼250 nm in diameter) is calculated to be ∼5 aF based on a simple parallel-plate model and thus its cutoff frequency is mainly limited by the transit time of the photogenerated charge carriers in the device, which may in principle[26] reach ∼100 GHz after certain parameter optimization.

Spectral photocurrent measurements to reveal the resonant photoresponse were performed with a chopped supercontinuum white light source (Fianium) coupled to a 0.25 m monochromator. The measured spectral external quantum efficiency (EQE) of a 280 nm diameter GeNW device biased at −1 V for randomly polarized, normal-incidence illumination is shown in Figure 2a. At a given wavelength, the EQE is defined as the ratio of the measured photocurrent and the photon flux in the projected area of a nanowire, i.e., the physical cross section of the nanowire as seen in a scanning electron microscope. For comparison, we also plot the EQE of a hypothetical 280 nm thick and 280 nm wide section at the surface of a bulk Ge wafer derived from the absorption coefficient of single-crystalline germanium[27] and assuming perfect carrier extraction. Distinct peaks in the nanowire's spectra can be seen at 800, 1050, and 1500 nm. Each peak results from the coupling to different transverse electric (TE_{ml}) and transverse magnetic (TM_{ml}) LMRs of the nanowire, where m and l are the azimuthal mode number and radial order of the resonances.[19] Good consistence between the experimental observation and theoretical results based on either the analytical Lorentz−Mie formalism[28] or full-field finite difference frequency domain (FDFD) further confirm that LMRs are at the origin of the peaks (see Figure S1 in Supporting Information). Whereas the analytical modeling allows for an easy association of the different photocurrent peaks to specific LMRs, the numerical simulations exhibit more accurate agreement with the experiments as they take into account the presence of the nanowire substrate. The analytic models indicate that the 800 nm peak mainly results

DOI: 10.1021/nl9037278 | *Nano Lett.* **2010,** *10,* 1229–1233

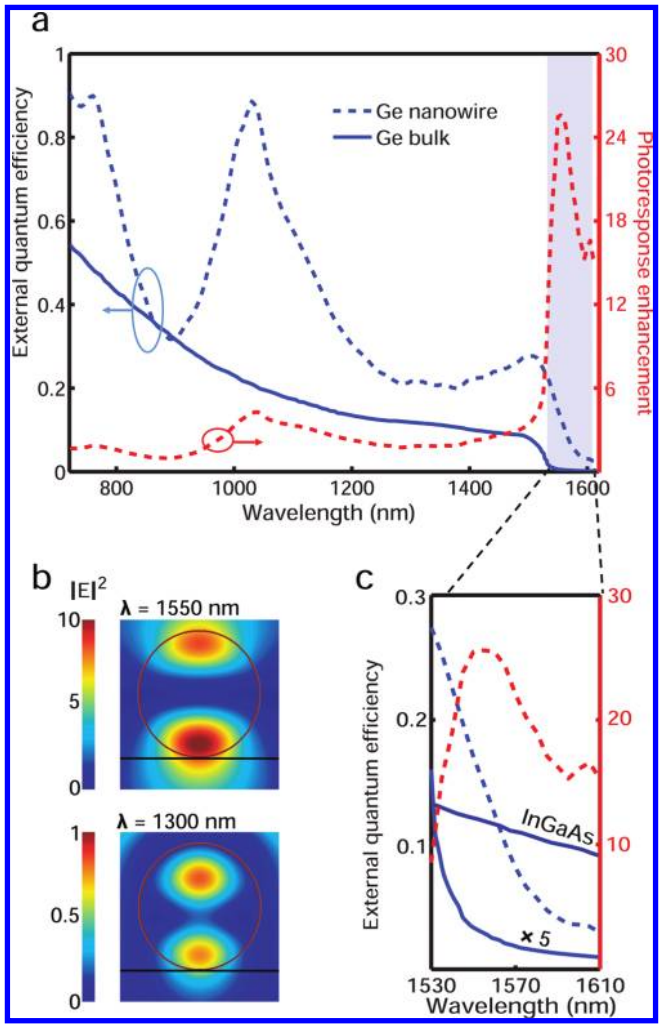

FIGURE 2. Enhanced EQE of Ge nanowire photodetectors. (a) Spectral dependence of the EQE for a 280 nm diameter Ge nanowire device (dashed blue line) and of bulk Ge without an antireflection coating and of comparable thickness (solid blue line) for unpolarized normal incidence. The data for the bulk were derived from the absorption coefficient in ref 27 and by assuming perfect carrier extraction. The dashed red line indicates the ratio between the EQEs of the nanowire and of the bulk, while the light purple bar highlights the wavelength region of interest in this paper, 1530−1610 nm. The spectral EQE of the nanowire photodetector depends on both the intrinsic absorption of Ge and the absorption enhancement caused by excitation of LMRs in the nanowire. By normalizing the EQE of the nanowire to that of a bulk Ge detector (the dashed red line), one can delineate the enhancement in absorption due to the optical resonances. (b) Distribution of the intensity of internal electric field inside the nanowire on resonance (upper) and off resonance (lower). Note the difference of 1 order of magnitude in the scale bar of $|E|^2$. (c) Expanded view of the highlighted photoresponses in (a), along with that of InGaAs, which is one of the most commonly used materials for commercial photodetectors in this wavelength.

from the TE_{21} and TM_{31} modes, the 1050 nm peak is due to the TE_{11} and TM_{21} modes, and the 1500 nm peak is related to the TE_{01} and TM_{11} modes (see Figure S2 in Supporting Information). At these resonances, the EQE in the nanowire is substantially larger than that in the bulk. Of particular importance is that the enhancement can be engineered to occur at the C-band (1530−1570 nm) and L-band (1570−1610 nm) communication wavelengths. An expanded view of the spectra in this region is shown in Figure 2c. The strong photoresponse of the NW device has been substantially extended on the long wavelength side and the entire C and L bands benefit from improvement by 1 order-of-magnitude over bulk Ge. It is important to note that the use of leaky mode resonances effectively extends the high-performance operation of Ge photodetectors to photon energies below the direct gap of Ge at 0.8 eV (i.e., wavelengths larger than 1550 nm). The photoresponse is even superior to much more expensive $In_{0.53}Ga_{0.47}As$,[29] one of the most commonly used materials for commercial photodetectors at this wavelength. Physically, the nanowire works as a cavity-antenna,[19,20] efficiently coupling the incident light to its LMRs and causing a strong buildup of electromagnetic field inside the absorbing semiconductor material. The effects of this type of resonance are clearly seen in a comparison of the simulated distribution of the electric field intensity on-resonance at a wavelength of 1550 nm and off-resonance at 1300 nm (note the 1 order-of-magnitude difference in the scale bar).

The nature of the LMRs not only dramatically enhances the photoresponse but also allows one to build valuable polarization and wavelength sensitive functions into the device, without the need for external components. Figure 3a shows measured polarization-selective spectra of the 280 nm diameter nanowire device. For the experiments, the incident light was linearly polarized with the electric field either parallel (TM) or perpendicular (TE) to the nanowire axis. The simulated ratio of the TM/TE photoresponse curves shows reasonable agreement with the experimental data. Figure 3b shows that for a given incident wavelength (1550 nm) the polarization dependence closely follows the expected $\cos^2 \phi$ behavior, where ϕ is the angle between the incident polarization and the nanowire axis. As indicated in Figure 3a, the EQE of the device for the TM polarized illumination is about twice (∼1.5−2-fold) as large as that for TE-polarized illumination in the wavelength range from 1.4 to 1.6 μm. As pointed out before, the absorption in this spectral region can mainly be attributed to the TM_{11} LMR (for TM-polarized incidence) and the TE_{01} LMR (for TE-polarized incidence). The 2-fold degeneracy of the TM_{11} mode explains the approximately twice as large photoresponse for TM-polarized light as compared to TE-polarized light, which couples to the nondegenerate TE_{01} mode.[19] Substrate effects cause some deviation from this ratio. Polarization anisotropy in the photoresponse of nanowire detectors has been reported before[30] but was not attributed to the nature of the LMRs. We believe the size- and wavelength- independent polarization anisotropy observed there is most likely because only the lowest order leaky mode TM_{01} could be excited given the small size of the nanowires. A deep understanding of the role of LMRs now allows for a rational design for photodetectors with an enhanced response and polarization-selective functionality at desired wavelengths. For example, without further optimization this

DOI: 10.1021/nl9037278 | *Nano Lett.* **2010,** *10,* 1229–1233

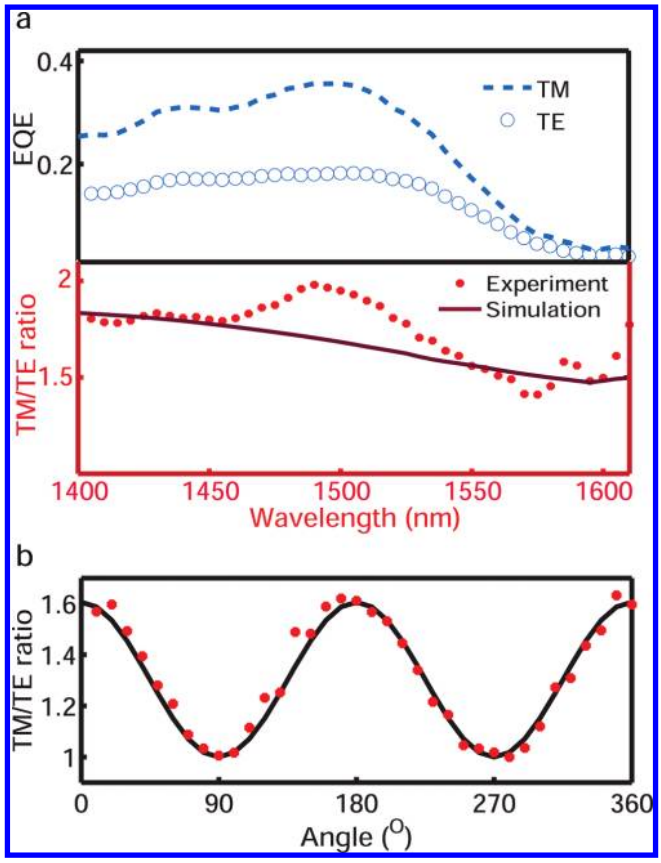

FIGURE 3. Polarization-sensitive photoresponse of the nanowire photodetector. (a) Lower, spectra of EQE of the 280 nm diameter nanowire for linearly polarized TM (dashed blue line) or TE (empty blue circles) light at normal incidence. Upper, the measured (dotted red line) and calculated (solid red line) ratio between the TM and TE quantum efficiencies. (b) Normalized photocurrent at a wavelength of 1550 nm as a function of the angle ϕ between the incident electric field and the nanowire axis. The solid line is a fit to a $\cos^2 \phi$ function.

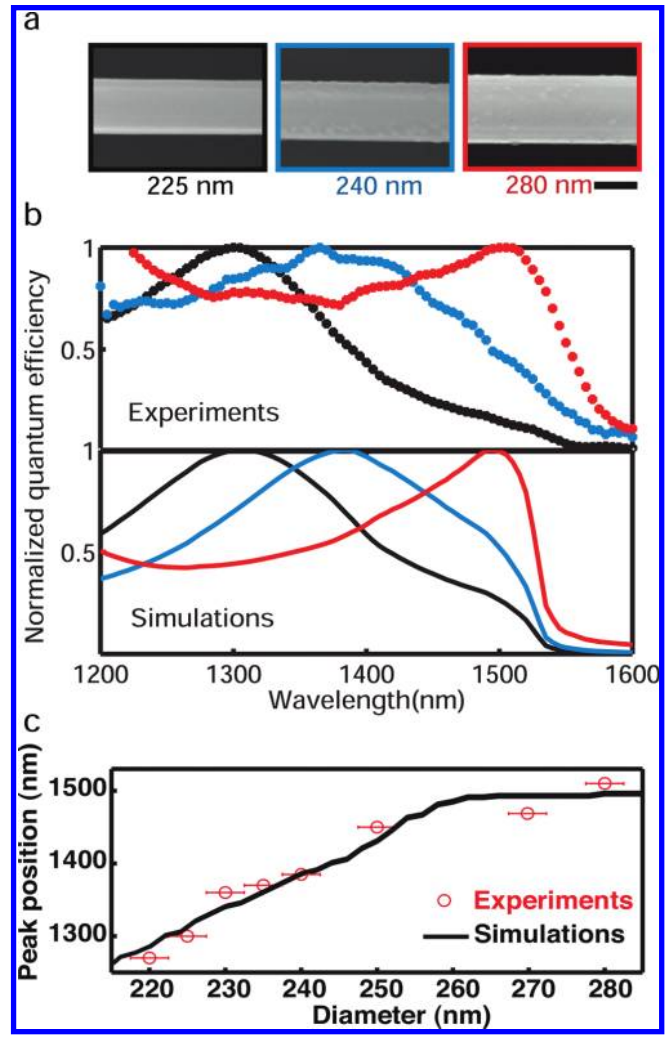

FIGURE 4. Wavelength-dependent photoresponse of different diameter Ge nanowire photodetectors. (a) SEM images of selected nanowires with diameters of 225, 240, and 280 nm used in the photodetectors (scale bar, 200 nm). (b) Normalized EQEs of the nanowire devices, measurements (upper) and simulations (lower). Each of the spectra was obtained by normalizing to its maximum EQE in the wavelength region from 1300−1600 nm. (c) Measured (red circle) and simulated (black solid) positions of the absorption peak in the near-infrared band as a function of nanowire diameter.

particular nanowire does not exhibit good polarization selective behavior at shorter wavelengths (see Supporting Information).

Figure 4 shows that optimal wavelength selectivity in the desired near-infrared optical communication band can be achieved through a thoughtful choice of nanowire diameter. Figure 4b shows experimental and simulated photoresponse spectra for the nanowires shown in Figure 4a. We can see that the photoresponse peak in this region shifts from 1300 to 1530 nm as the diameter of the nanowires is increased from 245 to 280 nm. The measurements are in very good agreement with the numerical simulations for these wire sizes. The measured peak position of photoresponse for a large number of measured nanowire devices is given in Figure 4c, along with the simulation results. These data show a monotonic dependence of the peak position on diameter, in agreement with the intuitive notion that resonances occur when the effective wavelength of the trapped photons in the wire fit an integer number of times around the circumference of the wire. This property, together with the ever-increasing control over nanostructure synthesis, opens tremendous opportunities for the realization of wavelength-selective detector arrays and imaging systems.

We have demonstrated a new method for rational design of compact Ge nanoantenna near-infrared photodetectors with a superior photoresponse, integrated wavelength and polarization selective functions, ultralow dark current, and low power dissipation. This high-performance nanometer-scale Ge photodetector represents a significant step forward toward building fully integrated optoelectronics circuits for on-chip communication. The use of LMRs in nanowires presents an exciting new paradigm for producing a variety of other novel miniaturized chipscale components, including high-performance lasers and modulators.

DOI: 10.1021/nl9037278 | Nano Lett. 2010, 10, 1229–1233

Acknowledgment. This work was sponsored by the Si-based Laser Initiative of the Multidisciplinary University Research Initiative (MURI) under the Air Force Aerospace Research OSR Award Number FA9550-06-1-0470 and supervised by LTC Gernot Pomrenke. Linyou Cao acknowledges the 2008 SPIE scholarship in Optical Science and Engineering.

Supporting Information Available. Figures showing external quantum efficiency. This material is available free of charge via the Internet at http://pubs.acs.org.

REFERENCES AND NOTES

(1) Barkai, A.; Chetrit, Y.; Cohen, O.; Cohen, R.; Elek, N.; Ginsburg, E.; Litski, S.; Michaeli, A.; Raday, O.; Rubin, D.; Sarid, G.; Izhaky, N.; Morse, M.; Dosunmu, O.; Liu, A.; Liao, L.; Rong, H.; Kuo, Y.; Xu, S.; Alduino, D.; Tseng, J.; Liu, H.; Paniccia, M. *J. Opt. Networking* **2007**, *6*, 25–47.
(2) Kirchain, R.; Kimerling, L. *Nat. Photonics* **2007**, *1*, 303–305.
(3) Pavesi, L.; Guillot, G. *Optical Interconnects: the Silicon Approach*; Springer: NewYork, 2006.
(4) Soref, R. A. *Proc. IEEE* **1993**, *81*, 1687–1706.
(5) Ahn, D.; Hong, C.; Liu, J.; Giziewicz, W.; Beals, M.; Kimerling, L. C.; Michel, J.; Chen, J.; Kartner, F. X. *Opt. Express* **2007**, *15*, 3916–3921.
(6) Chen, L.; Dong, P.; Lipson, M. *Opt. Express* **2008**, *16*, 11513–11518.
(7) Dosunmu, O. I.; Cannon, D. D.; Emsley, M. K.; Ghyselen, B.; Liu, J.; Kimerling, L. C.; Ünlü, M. S. *IEEE J. Sel. Top. Quantum Electron.* **2004**, *10*, 694–701.
(8) Sahni, S.; Luo, X.; Liu, J.; Xie, Y.; Yablonovitch, E. *Opt. Lett.* **2008**, *33*, 1138–1140.
(9) Tang, L.; Kocabas, S. E.; Latif, S.; Okyay, A. K.; Ly-Gagnon, D.; Saraswat, K. C.; Miller, D. A. B. *Nat. Photonics* **2008**, *2*, 226–229.
(10) Yin, T.; Cohen, R.; Morse, M. M.; Sarid, G.; Chetrit, Y.; Rubin, D.; Paniccia, M. J. *Opt. Express* **2007**, *15*, 13965–13971.
(11) White, J. S.; Veronis, G.; Yu, Z.; Barnard, E. S.; Chandran, A.; Fan, S.; Brongersma, M. L. *Opt. Lett.* **2009**, *34*, 686–688.
(12) Falk, A. L.; Koppens, F. H. L.; Yu, C. L.; Kang, K.; Snapp, N. d. L.; Akimov, A. V.; Jo, M. H.; Lukin, M. D.; Park, H. *Nat. Phys.* **2009**, *5*, 475–479.
(13) Antoni, T.; Nedelcu, A.; Marcadet, X.; Facoetti, H.; Berger, V. *Appl. Phys. Lett.* **2007**, *90*, 20110.
(14) Chen, E.; Chou, S. Y. *Elec. Lett.* **1996**, *32*, 1510–1511.
(15) Ramam, A.; Chowdhury, G. K.; Chua, S. J. *Appl. Phys. Lett.* **2005**, *86*, 171104.
(16) Tokuda, T.; Sato, S.; Yamada, H.; Sasagawa, K.; Ohta, J. *Electron. Lett.* **2009**, *45*, 228–230.
(17) Govindarajan, M.; Forrest, S. R.; Cheng, L.; Sawchuk, A. A. *IEEE Photonics Technol. Lett.* **1991**, *3*, 669–672.
(18) Alexander, S. A. *Optical Communication Receiver Design*; SPIE: Bellingham, WA, 1997.
(19) Cao, L.; White, J. S.; Park, J. S.; Clemens, B. M.; Schuller, J. A.; Brongersma, M. L. *Nat. Mater.* **2009**, *8*, 643—647.
(20) Cao, L.; Fan, P.; Vasudev, A. P.; White, J. S.; Yu, Z.; Cai, W.; Schuller, J. A.; Fan, S.; Brongersma, M. L. *Nano Lett.* **2010**, *10*, 439–445.
(21) Cao, L.; Nabet, B.; Spanier, J. E. *Phys. Rev. Lett.* **2006**, *96*, 157402.
(22) Muskens, O. L.; Diedenhofen, S. L.; Kaas, B. C.; Algra, R. E.; Bakkers, E. P. A. M.; Rivas, J. G.; Lagendijk, A. *Nano Lett.* **2008**, *9*, 930–934.
(23) Long, S. A.; McAllister, M. K. *IEEE Trans. Antennas Propag.* **1983**, *Ap-31*, 406–412.
(24) Wang, D.; Dai, H. *Appl. Phys. A: Mater. Sci. Process.* **2006**, *85*, 217–225.
(25) Chui, C. O.; Okyay, A. K.; Saraswat, K. C. *IEEE Photonics Technol. Lett.* **2003**, *15*, 1585–1587.
(26) Chen, J. W.; Kim, D. K.; Das, M. B. *IEEE Trans. Electron Devices* **1996**, *43*, 1838–1843.
(27) Palik, E. D. *Handbook of Optical Constants of Solids*; Acadmic Press: London, 1985.
(28) Bohren, C. F.; Huffman, D. R. *Absorption and Scattering of Light by Small Particles*; John Wiley & Sons, Inc.: New York, 1998.
(29) Adachi, S. *Physical properties of III-V Semiconductor Compounds*; Wiley-VCH: New York, 1992.
(30) Wang, J.; Gudiksen, M. S.; Duan, X.; Cui, Y.; Lieber, C. M. *Science* **2001**, (293), 1455–1457.

DOI: 10.1021/nl9037278 | *Nano Lett.* **2010,** *10,* 1229–-1233